J|A|C|S
ARTICLES
Published on Web 03/20/2002

Temperature-Dependent Isotope Effects in Soybean Lipoxygenase-1: Correlating Hydrogen Tunneling with Protein Dynamics

Michael J. Knapp, Keith Rickert,† and Judith P. Klinman*

Contribution from the Department of Chemistry and Department of Molecular and Cell Biology, University of California, Berkeley, California 94720

Received September 19, 2001

Abstract: The hydrogen-atom transfer in soybean lipoxygenase-1 (SLO) exhibits a large kinetic isotope effect on k_{cat} (KIE = 81) near room temperature and a very weak temperature dependence (E_{act} = 2.1 kcal/mol). These properties are consistent with H· transfer that occurs entirely by a tunneling event. Mutants of SLO were prepared, and the temperature dependence of the KIE was measured, to test for alterations in the tunneling behavior. All mutants studied exhibit KIEs of similar, large magnitude at 30 °C, despite an up to 3 orders of magnitude change in k_{cat}. E_{act} for two of the mutants (Leu^{754} → Ala, Leu^{546} → Ala) is larger than for wild-type (WT), and the KIE becomes slightly more temperature dependent. In contrast, Ile^{553} → Ala exhibits k_{cat} and E_{act} parameters similar to wild-type soybean lipoxygenase-1 (WT-SLO) for protiated substrate; however, the KIE is markedly temperature dependent. The behavior of the former two mutants could reflect increased reorganization energies (λ), but the behavior of the latter mutant is inconsistent with this description. We have invoked a full H· tunneling model (Kuznetsov, A. M.; Ulstrup, J. *Can. J. Chem.* **1999**, *77*, 1085−1096) to explain the temperature dependence of the KIE, which is indicative of the extent to which distance sampling (gating) modulates hydrogen transfer. WT-SLO exhibits a very small E_{act} and a nearly temperature-independent KIE, which was modeled as arising from a compressed hydrogen transfer distance with little modulation of the hydrogen transfer distance. The observations on the Leu^{754} → Ala and Leu^{546} → Ala mutants were modeled as arising from a slightly less compressed active site with greater modulation of the hydrogen transfer distance by environmental dynamics. Finally, the observed behavior of the Ile^{553} → Ala mutant indicates a relaxed active site with extensive involvement of gating to facilitate hydrogen transfer. We conclude that WT-SLO has an active site structure that is well organized to support hydrogen tunneling and that mutations perturb structural elements that support hydrogen tunneling. Modest alterations in active site residues increase λ and/or increase the hydrogen transfer distance, thereby affecting the probability that tunneling can occur. These studies allow the detection and characterization of a protein-gating mode in catalysis.

Introduction

The study of enzyme catalysis has led to many proposals for how catalysts work, the most basic of which is Pauling's concept of transition-state stabilization.[1] Transition-state stabilization postulates that catalysts work by reducing the height ($\Delta G^{\ddagger}$) of the potential energy barrier that must be overcome to effect catalysis. Recent attention, however, has turned to the role of hydrogen tunneling through this potential energy barrier, implicating barrier width as an important component of catalytic efficiency.[2−8] Furthermore, modulation of potential energy barriers through environmental oscillations may play an important role in hydrogen tunneling reactions.[9−13] Hydrogen tunneling is very sensitive to the reaction barrier shape and, as such, can report on changes in this barrier directly. Some of the most compelling evidence for tunneling effects in an enzymatic reaction has come from the hydrogen atom (H·) abstraction catalyzed by soybean lipoxygenase-1 (SLO).[5,14−18]

* To whom correspondence should be addressed. E-mail: klinman@socrates.berkeley.edu.
† Present address: Merck & Co., Inc., Department of Cancer Research, WP42-300, West Point, PA 19486.

(1) Kraut, J. *Science* **1988**, *242*, 533−539.
(2) Kohen, A.; Klinman, J. P. *Acc. Chem. Res.* **1998**, *31*, 397−404.
(3) Kohen, A.; Klinman, J. P. *Chem. Biol.* **1999**, *6*, R191−R198.
(4) Sutcliffe, M. J.; Scrutton, N. S. *Trends Biochem. Sci.* **2000**, *25*, 405−408.
(5) Glickman, M. H.; Wiseman, J. S.; Klinman, J. P. *J. Am. Chem. Soc.* **1994**, *116*, 793−794.
(6) Cha, Y.; Murray, C. J.; Klinman, J. P. *Science* **1989**, *243*, 1325−1330.
(7) Bahnson, B. J.; Colby, T. D.; Chin, J. K.; Goldstein, B. M.; Klinman, J. P. *Proc. Natl. Acad. Sci. U.S.A.* **1997**, *94*, 12797−12802.
(8) Bahnson, B. J.; Klinman, J. P. *Methods Enzymol.* **1995**, *249*, 373−397.
(9) Antoniou, D.; Schwartz, S. D. *Proc. Natl. Acad. Sci. U.S.A.* **1997**, *94*, 12360−12365.
(10) Borgis, D. C.; Lee, S. Y.; Hynes, J. T. *Chem. Phys. Lett.* **1989**, *162*, 19−26.
(11) Bruno, W. J.; Bialek, W. *Biophys. J.* **1992**, *63*, 689−699.
(12) Kohen, A.; Cannio, R.; Bartolucci, S.; Klinman, J. P. *Nature* **1999**, *399*, 496−499.
(13) Kuznetsov, A. M.; Ulstrup, J. *Can. J. Chem.* **1999**, *77*, 1085−1096.
(14) Glickman, M. H.; Klinman, J. P. *Biochemistry* **1995**, *34*, 4, 14077−14092.
(15) Glickman, M. H.; Klinman, J. P. *Biochemistry* **1996**, *35*, 12882−12892.
(16) Glickman, M. H.; Cliff, S.; Thiemens, M.; Klinman, J. P. *J. Am. Chem. Soc.* **1997**, *119*, 11357−11361.
(17) Jonsson, T.; Glickman, M. H.; Sun, S. J.; Klinman, J. P. *J. Am. Chem. Soc.* **1996**, *118*, 10319−10320.
(18) Rickert, K. W.; Klinman, J. P. *Biochemistry* **1999**, *38*, 12218−12228.

10.1021/ja012205t CCC: $22.00

SLO catalyzes the production of fatty acid hydroperoxides at 1,4-pentadienyl positions, and the product 13-(*S*)-hydroperoxy-9,11-(*Z*,*E*)-octadecadienoic acid (13-(*S*)-HPOD) is formed from the physiological substrate linoleic acid (9,12-(*Z*,*Z*)-octadecadienoic acid) (LA). This reaction proceeds by an initial, rate-limiting abstraction of the pro-*S* hydrogen atom (H·) from C-11 of LA by the Fe^{3+}-OH cofactor, forming a substrate-derived radical intermediate and Fe^{2+}-OH_2. Molecular oxygen rapidly reacts with this radical, eventually forming 13-(*S*)-HPOD and regenerating resting enzyme. The steady-state rate of catalysis[5] (k_{cat}) shows similar properties as single-turnover[17] experiments, in support of the H· abstraction step limiting both measurements. Previous experiments ruled out potential complications, such as magnetic field effects[19] or reaction branching,[14] as the origin of the large kinetic isotope effect on k_{cat} (KIE). The sum of the data is consistent with the measured KIE reflecting an intrinsic KIE for a single chemical step. SLO turnover exhibits weak temperature dependence ($E_{act} = 2.2$ kcal/mol), a small Arrhenius prefactor ($A_H < 10^5$ s^{-1}), and large KIE on k_{cat} ($^Dk_{cat} = 81$).[18] Additionally, the KIE is close to temperature independent, leading to a large isotope effect on the Arrhenius prefactor, $A_H/A_D \gg 1$.[17,18]

Each of these parameters for SLO, $^Dk_{cat}$, E_{act}, and A_H/A_D is inconsistent with the transition-state theory (TST) view of catalysis. The activation energy is so low as to be meaningless within a simple TST model, implying that virtually all of the rate acceleration for this C−H bond cleavage is entropic in origin, and both the KIE and A_H/A_D far exceed classical predictions. Additionally, A_H is reduced from the TST-prediction of $A_{TST} = 10^{13}$ s^{-1}, suggesting that the reaction can be described as nonadiabatic.[20,21] Many workers have shown that nonclassical KIE behavior, such as $A_H/A_D \neq 1$, large KIEs, or deviations of the Swain−Schaad relationship from classical predictions,[8,12] reflects different degrees of hydrogen tunneling.[2,6,12,22,23] In this context, hydrogen tunneling in a static environment has been invoked to explain the properties of SLO.[14] However, this is unsatisfactory, since a simple static tunneling model predicts[24] an enormous KIE (ca. 10^3) and an $E_{act} = 0$.

Several theoretical groups have proposed models for hydrogen-isotope transfer that start from the reasonable premise that H· transfers are fully quantum-mechanical events (H/D/T tunneling) that are modulated by the environment.[10,11,13,25] This approach treats the hydrogen transfer as being fully nonclassical, in contrast to the tunnel correction models which lead to partial nonclassical behavior. Environmental coupling leads to the observed Arrhenius-like behavior in hydrogen transfers, through both a Marcus-like activation energy, and an environmental vibration (gating) that modulates the H· transfer distance. The Marcus term reflects thermal activation due to fluctuations within the environmental coordinate, as in electron-transfer theory, leading to Arrhenius-like rates ($\ln k \propto 1/T$) but to KIEs that are close to temperature independent. Gating introduces an additional temperature-dependent factor to the rates, by modulating the distance for hydrogen transfer. Thus, the temperature dependence of the KIE will reflect the relative contribution of the reorganization energy and gating to the reaction coordinate. This is a significant departure from classical reaction models that ignore the coupling of dynamics to the bond-cleavage coordinate.

SLO is an ideal enzyme to test the applicability of this environmentally modulated H· transfer model. Its kinetic properties are so deviant from those predicted by classical models that a full tunneling model is required. In this paper, we describe the use of site-directed mutagenesis in which each of several bulky, hydrophobic residues within the active site of SLO has been replaced by alanine. The effect of this reduced bulk on the environmental modulation of H· tunneling has been probed by variable-temperature KIE measurements. Wild-type soybean lipoxygenase-1 (WT-SLO) exhibits nearly temperature-independent KIEs and a small E_{act}, consistent with a reaction coordinate that is dominantly controlled by the environmental reorganization energy. Moderately temperature-dependent KIEs and an increased E_{act} are observed for those point mutations closest to the Fe^{3+}-OH, $Leu^{546} \rightarrow$ Ala and $Leu^{754} \rightarrow$ Ala. These observations are attributed primarily to an increased environmental reorganization energy that controls tunneling via the Marcus-term, with a moderate contribution of gating to the reaction coordinate. Mutation of a more distal position, $Ile^{553} \rightarrow$ Ala, produces the curious behavior that H· transfer is unaltered, while the KIE becomes very temperature dependent. These observations require that the thermally active gating term contributes extensively to the reaction coordinate, modulating the transfer distance and D· tunneling probability.[3,10,11,13] This analysis allows the separation of "passive dynamics", parametrized by the environmental reorganization term (λ), from "active dynamics", which modulates the hydrogen tunneling barrier. Importantly, the results described herein lead to a new formalism for the interpretation of the temperature dependence of isotope effects in enzyme-catalyzed H· transfers.

Materials and Methods

Mutagenesis and Protein Purification. All proteins were expressed on the pT7-7 plasmid in *E. coli* and purified as described previously.[18,26] Mutants were prepared using the Stratagene Quickchange protocol.[18] The $Leu^{546} \rightarrow$ Ala mutation was confirmed by sequencing the mutant plasmid over a ~100 bp region centered on the mutation site.[18] The $Ile^{553} \rightarrow$ Ala and $Leu^{754} \rightarrow$ Ala mutations were confirmed by sequencing the mutant plasmids over a ~500 bp region containing the mutation site.[27]

Kinetics Measurements. Steady-state kinetics were performed on a single-wavelength UV spectrophotometer by measuring the initial, linear rate of 13-(*S*)-HPOD formation ($\epsilon_{234} = 23\,600$ M^{-1} cm^{-1}).[18] All assays were performed in 0.1 M Borate buffer (pH 9.00) in a thermally jacketed cuvette under an ambient atmosphere. Linoleic acid stock solutions (ca. 1 mM) were prepared as previously described.[18] Stock linoleic acid concentrations were determined spectrophotometrically, by enzymatically converting substrate to product. Kinetic assays were performed at 1−80 μM LA for WT-SLO, $Leu^{546} \rightarrow$ Ala, and $Ile^{553} \rightarrow$ Ala; $Leu^{754} \rightarrow$ Ala was assayed at 1−20 μM LA, as substrate inhibition was noted above 20 μM LA. Initial rates were fit to the Michaelis−Menten equation ($v = k_{cat}[S]/(K_M + [S])$) to obtain the kinetic

(19) Hwang, C. C.; Grissom, C. B. *J. Am. Chem. Soc.* **1994**, *116*, 795−796.
(20) Cukier, R. I.; Nocera, D. G. *Annu. Rev. Phys. Chem.* **1998**, *49*, 337−369.
(21) Westphal, K. L.; Tommos, C.; Cukier, R. I.; Babcock, G. T. *Curr. Opin. Plant Biol.* **2000**, *3*, 236−242.
(22) Basran, J.; Sutcliffe, M. J.; Scrutton, N. S. *Biochemistry* **1999**, *38*, 3218−3222.
(23) Scrutton, N. S.; Basran, J.; Sutcliffe, M. J. *Eur. J. Biochem.* **1999**, *264*, 666−671.
(24) Moiseyev, N.; Rucker, J.; Glickman, M. H. *J. Am. Chem. Soc.* **1997**, *119*, 3853−3860.
(25) Borgis, D.; Hynes, J. T. *Chem. Phys.* **1993**, *170*, 315−346.
(26) Holman, T. R.; Zhou, J.; Solomon, E. I. *J. Am. Chem. Soc.* **1998**, *120*, 0, 12564−12572.
(27) U.C. Berkeley DNA Sequencing Facility.

parameters k_{cat} and k_{cat}/K_M; standard errors from the fit are reported.[28] Standard errors from these fits were used to weight the Arrhenius fits. Rate constants were corrected for the iron content of each enzyme preparation.[29] Noncompetitive isotope effects were obtained by using $^1H_{31}$-LA and either 11,11-$^2H_2$-LA (WT, Leu^{546} → Ala, Ile^{553} → Ala) or $^2H_{31}$-LA as substrates. Previous studies have shown little difference in isotope effect using either 11,11-$^2H_2$-LA or $^2H_{31}$-LA.[18] The synthesis of 11,11-$^2H_2$-LA is detailed elsewhere.[18] The reported KIE is then the ratio of the rates of H· abstraction to D· abstraction (KIE = $^Dk_{cat}$ = $k_{cat}H/k_{cat}D$). Data for Leu^{546} → Ala appeared in an earlier publication[18] concerned with measuring the 2° KIE, but were not analyzed in detail for effects on the primary tunneling events.

All data presented herein were obtained under an ambient atmosphere (20.8% O_2) and corrected to O_2 saturation as needed. Because SLO is a bisubstrate enzyme, k_{cat} refers to the conditions under which both LA and O_2 are saturating. These conditions were met under an ambient atmosphere for all experiments using deutero-linoleic acid, as $K_{M(O2)} < 10\mu$M, and ambient $[O_2] \geq 200\ \mu$M over the 10−50 °C temperature range. This condition was also met for $^1H_{31}$-LA with both Leu^{546} → Ala and Leu^{754} → Ala mutants, again due to a low $K_{M(O2)}$. However, a correction was required for WT-SLO and Ile^{553} → Ala, as these enzymes show $K_{M(O2)} \approx 20-50\ \mu$M over the range of temperatures investigated. The effect of subsaturating O_2 was accounted for by comparing the apparent k_{cat} (k_{cat}(app)) obtained under an ambient atmosphere (approximately 20.8% O_2) to that obtained under an atmosphere of 100% O_2, and then correcting the ambient rates. This amounted to a correction of a few percent at each temperature for WT-SLO and Ile^{553} → Ala and had only minor effects on the kinetic parameters describing k_{cat} and the derived isotope effects. The uncorrected and corrected data are shown together in a Supporting Information figure.

Simulations. Analytical rate expressions for gated hydrogen tunneling were used to calculate the variable-temperature rates and isotope effects in SLO. The H· transfer of SLO was assumed to have a very weak electronic coupling (electronically nonadiabatic) and to be nonadiabatic in the hydrogen coordinate due to the absence of significant hydrogen bonding. The assumption of electronic nonadiabaticity is likely an oversimplification; however, it will not affect our conclusions that are based on the temperature dependence of isotope effects. The fully nonadiabatic approach of Kuznetsov and Ulstrup[13] was used to model the data.

Rate expressions within the nonadiabatic limit take the form of a modified Fermi's Golden Rule expression (eq 1), which has direct analogues to those obtained for electron-transfer reactions in which a single quantum mode (the C−H stretch) has been separated from the classical environmental coordinate.[30] The rate is a sum over all level-specific rates, in which υ is the vibrational quantum number for reactant, and w is the vibrational quantum number for product, that have been normalized for the thermal populations (P_υ). The rate is determined by $|V_{el}|^2$, the electronic overlap of reactant and product squared, and an environmental energy term relating λ, the reorganization energy of classical modes, to $\Delta G°$, the driving force for the reaction, and E_{vib}, which is the vibrational energy difference between product and reactant. The hydrogen stretch is treated quantum mechanically, and its contribution to the rate is due to a vibration-level specific Franck−Condon nuclear overlap (F.C. term). Other symbols have their usual meaning: k_b is Boltzmann's constant, $\hbar$ is Planck's constant divided by 2π, and R and T are the gas constant and absolute temperature, respectively. A brief derivation of eq 1 that follows from Kuznetsov and Ulstrup[13] is shown in the Appendix.

$$k_{tun} = \sum_{\upsilon} P_\upsilon \sum_{w} \frac{1}{2\pi} |V_{el}|^2 \sqrt{4\pi^3/\lambda RT\hbar^2}\ \exp^{-(\Delta G°+E_{vib}+\lambda)^2/(4\lambda RT)} \times (\text{F.C. term})_{\upsilon,w} \quad (1)$$

The isotope dependence within the fully nonadiabatic model arises entirely from the F.C. term, which determines the tunneling probability of hydrogen. Vibration-level specific Franck−Condon overlaps have been previously described,[31] with the overlap for the $\upsilon = 0 \rightarrow w = 0$ transition explicitly shown in eq 2a; all other F.C. terms are explicitly shown in the Appendix. This nuclear overlap depends on the frequency (ω_H) and mass (m_H) of the oscillator, as well as Δr, the separation between the minima of the initial and final wells along the hydrogen coordinate. Oscillators of equal mass were assumed here, as the reduced mass of an OH and a CH oscillator are very similar ($\mu_{OH} \approx \mu_{CH} = 0.923$ g/mol; $\mu_{OD} \approx \mu_{CD} = 1.71$ g/mol). Likewise, equal vibrational frequencies were assumed ($\nu_{CH,OH} = 3000\ cm^{-1}$; $\nu_{CD,OD} = 2200\ cm^{-1}$).

$$\text{F.C. term}_{0,0} = (\exp^{-m_H\omega_H\Delta r^2/2\hbar}) \quad (2a)$$

$$\text{F.C. term}_{0,0} = \int_0^{r_0} (\exp^{-m_H\omega_H\Delta r^2/2\hbar}) \exp^{-\hbar\omega_X X^2/2RT}\, dX \quad (2b)$$

A small temperature dependence to the isotope effects arises from thermal populations of the hydrogen (or deuterium) vibrational levels. Overlap between the lowest two reactant vibrational levels ($\upsilon = 0,1$) and the lowest four product vibrational levels ($w = 0,1,2,3$) was included in the calculations; the offset of vibrational energies between reactant and product was accounted for by the E_{vib} term in eq 1. Thus, this model accounted for transfer to excited vibrational states of product, as well as the small amount of thermal excitation to the reactants first excited vibrational level. In the case of protium, ground-state transitions ($0 \rightarrow 0$) accounted for greater than 95% of tunneling in the 270−320 K temperature range, while deuterium tunneling involved excited states ($0 \rightarrow 1$, $1 \rightarrow 1$) to an appreciable degree (see Supporting Information for details).

Because of the strong distance dependence of the hydrogen coupling, environmental oscillations can appreciably alter the hydrogen overlap.[32] The effective stretch between the donor and acceptor (C−H- - -O−Fe) was included in the resultant F.C. term to account for this dynamically modulated tunneling distance (eq 2b). These environmental dynamics lead to changes in the KIE; Borgis and Hynes[10,25,32] refer to this coordinate as "Q", while Kuznetsov and Ulstrup[13] denote this classical gating coordinate "X". The resultant transfer distance ($\Delta r = r_0 - r_X$) is reduced from the equilibrium separation (r_0) by the distance of gating (r_X). X is a reduced coordinate, which was defined by $X = r_X\sqrt{m_X\omega_X/\hbar}$, where m_X is the mass and ω_X the classically treated frequency of the gating coordinate.

Results

Kinetics. The rate of catalysis (k_{cat}) for WT-SLO and the Ile^{553} → Ala mutant between 5° and 50 °C is shown in Figure 1, for both H· and D· abstraction. Prior work has shown that k_{cat} is limited by the rate of H· (or D·) abstraction, and therefore reflects only this chemical step.[18] The temperature dependencies of k_{cat} for both H· and D· abstraction were fitted with the empirical Arrhenius equation ($k = A\ \exp^{-E_{act}/RT}$) to obtain E_{act} and the Arrhenius prefactor, A. The rates and activation energies for H· abstraction for WT-SLO and Ile^{553} → Ala are similar to each other (Table 1); the difference between these enzymes becomes apparent in the change in activation energy for D· versus H· abstraction ($\Delta E_{act} = E_{act}D - E_{act}H$), where ΔE_{act} has increased ca. 4-fold.

In contrasting the behavior of WT-SLO and Ile^{553} → Ala, it can be seen that the Ile^{553} → Ala mutant has a more temperature-dependent KIE (Figure 1). The activation energy for D·

(28) *KaleidaGraph*; Synergy Software.
(29) Knapp, M. J.; Seebeck, F. P.; Klinman, J. P. *J. Am. Chem. Soc.* **2001**, *123*, 2931−2932.
(30) Marcus, R. A.; Sutin, N. *Biochim. Biophys. Acta* **1985**, *811*, 265−322.
(31) Ulstrup, J.; Jortner, J. *J. Chem. Phys.* **1975**, *63*, 4358−4368.
(32) Borgis, D.; Hynes, J. T. *J. Phys. Chem.* **1996**, *100*, 1118−1128.

Table 1. Kinetic Parameters for SLO and Mutants in pH 9.0 Borate Buffer[a]

	k_{cat}[b] (s^{-1})	KIE[c]	E_{act} (kcal/mol)	ΔE_{act}[d] (kcal/mol)	A_H (s^{-1})	A_H/A_D	k_{cat}/K_M[b] ($\mu M^{-1} s^{-1}$)	$\Delta\Delta G_T^{\ddagger}$ (kcal/mol)
WT-SLO[e]	297 (12)	81 (5)	2.1 (0.2)	0.9 (0.2)	9×10^3 (2×10^3)	18 (5)	11 (1)	
$Leu^{546} \rightarrow Ala$[e]	4.8 (0.6)	93 (9)	4.1 (0.4)	1.9 (0.6)	4×10^4 (3×10^4)	4 (4)	0.33 (0.1)	−2.1 (0.1)
$Leu^{754} \rightarrow Ala$	0.31 (0.02)	112 (11)	4.1 (0.3)	2.0 (0.5)	2×10^2 (1×10^2)	3 (3)	0.07 (0.02)	−3.0 (0.1)
$Ile^{553} \rightarrow Ala$	280 (10)	93 (4)	1.9 (0.2)	4.0 (0.3)	7×10^3 (2×10^3)	0.12 (0.06)	12 (1)	−0.05 (0.02)

[a] Data were collected between 5 and 50 °C. [b] The rate constants (k_{cat} and k_{cat}/K_M using $^1H_{31}$-LA) are reported for 30 °C. [c] KIE = $^Dk_{cat} = k_{cat}H/k_{cat}D$. [d] This is the isotope effect on E_{act}, $\Delta E_{act} = E_{act}D - E_{act}H$. [e] Rickert, K. W.; Klinman, J. P. *Biochemistry* **1999**, *38*, 12218−12228.

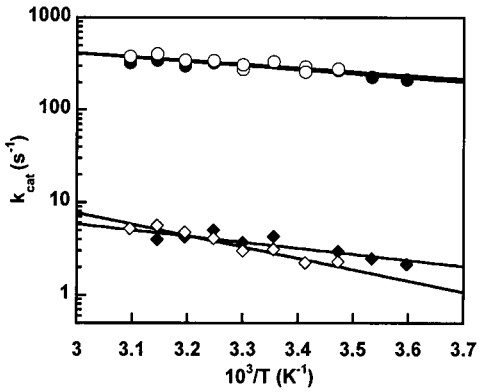

Figure 1. Arrhenius plot of kinetic data for WT-SLO (filled symbols) and $Ile^{553} \rightarrow Ala$ (open symbols) using protio-linoleic acid (circles) and deutero-linoleic acid (diamonds). The data for points for WT-SLO and $Ile^{553} \rightarrow Ala$ using protio-linoleic acid (circles) are superimposed between $10^3/T = 3.2, 3.5$; therefore, the filled circles are not visible. Nonlinear fits to the Arrhenius equation are shown as solid lines; error bars are obscured by the symbols.

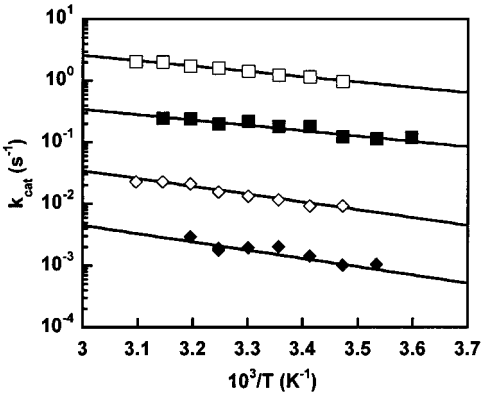

Figure 2. Arrhenius plot of kinetic data for $Leu^{546} \rightarrow Ala$ (open symbols) and $Leu^{754} \rightarrow Ala$ (closed symbols) using protio-linoleic acid (squares) and deutero-linoleic acid (diamonds). Nonlinear fits to the Arrhenius equation are shown as solid lines; error bars are obscured by the symbols.

abstraction by WT-SLO has a temperature dependence that is similar to that for H· abstraction (ΔE_{act} is small), leading to a KIE that is nearly temperature independent. Consequently, the value for the isotope effect on the Arrhenius prefactor is significantly above unity for WT-SLO; $A_H/A_D \gg 1$. On the other hand, the mutant $Ile^{553} \rightarrow Ala$ has a significantly more temperature-dependent rate for D· abstraction than for H· abstraction (ΔE_{act} is large), leading to an isotope effect on the Arrhenius prefactor that is below unity; $A_H/A_D \ll 1$.

Kinetic data for two other mutants, $Leu^{546} \rightarrow Ala$ and $Leu^{754} \rightarrow Ala$, are shown in Figure 2 and are summarized in Table 1. These show significantly reduced rates relative to WT-SLO, together with increased values for E_{act}. Despite these changes, the magnitude of the KIE at 30 °C remains similar to that of WT-SLO. As with the $Ile^{553} \rightarrow Ala$ mutant, the magnitude of

Scheme 1. Chemical Reaction of Soybean Lipoxygenase-1

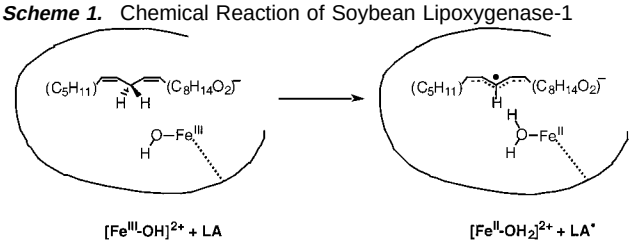

Scheme 2. Calculated O−H Bond Strength in Reduced Soybean Lipoxygenase-1

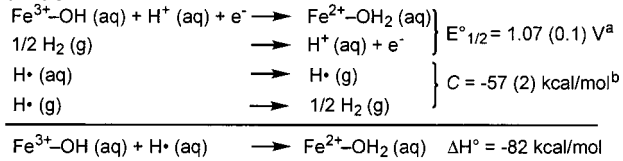

[a] The standard reduction potential for SLO (at pH = 0) is $E°_{1/2} = 0.6 (0.1) + 0.059 \times 8 = 1.07 (0.1)$ V. This results in a calculated $\Delta G° = -nFE° = -24.7$ kcal/mol. [b] $C = \Delta H°\{H\cdot (aq) \rightarrow H\cdot (g)\} + \Delta H°\{H\cdot (g) \rightarrow {}^1/_2H_2 (g)\} - {}^1/_2TS°\{H_2 (g)\}$. The constant C was taken from ref 33, and converts an aqueous reduction potential to an aqueous bond enthalpy. The final value for C also takes into account the conversion of $\Delta G°$, calculated from the standard reduction potential ($E°_{1/2}$), into $\Delta H°$. This latter process assumes equal entropy for $Fe^{3+}-OH$ (aq) and $Fe^{2+}-OH_2$ (aq), leading to the relationship $\Delta H° = \Delta G° - TS° \{{}^1/_2H_2 (g)\}$.

A_H/A_D is reduced from that of WT-SLO; however, it is above unity ($A_H/A_D \approx 3$). This reflects a more temperature-dependent isotope effect than that observed in WT-SLO, an effect that is also evident in the roughly 2-fold increase in ΔE_{act} from WT-SLO. It appears that WT-SLO and the three mutants form a series in which the isotope effect becomes more temperature dependent in the order WT < $Leu^{546} \rightarrow Ala$, $Leu^{754} \rightarrow Ala$ < $Ile^{553} \rightarrow Ala$.

Driving Force for H· Abstraction. The driving force for H· abstraction was estimated from the net change in bond dissociation energies (BDEs)[33] of the bonds formed (Fe^{2+}-(OH)−H) and broken (R_2CH-H) in the reaction catalyzed by SLO (Scheme 1).

The BDE for the newly formed O−H bond in Fe^{2+}-OH_2 was calculated (Scheme 2) to be 82 kcal/mol by assuming that the reported[34] redox potential for SLO, $E_{1/2} = 0.6 (0.1)$ V (vs NHE) at pH 8.0, is proton-coupled. By using the reported BDE (76 kcal/mol) for the pentadienyl[35] C−H bond of linoleic acid and the assumption that the entropy change upon reaction is negligible, a value of $\Delta G° = -6$ kcal/mol for the reaction in Scheme 1 is obtained.

Simulations. The underlying assumption in these simulations is that hydrogen transfer always occurs by environmentally modulated hydrogen tunneling. To gain insight into the effect

(33) Mayer, J. M. *Acc. Chem. Res.* **1998**, *31*, 441−450.
(34) Nelson, M. J. *Biochemistry* **1988**, *27*, 4273−4278.
(35) McMillen, D. F.; Golden, D. M. *Annu. Rev. Phys. Chem.* **1982**, *33*, 493−532.

Table 2. Input Parameters (Left), and Calculated Kinetic Isotope Effects (Right), for SLO and Mutants in the Environmentally Coupled Hydrogen Tunneling Model

	$-\Delta G°$ (kcal/mol)	λ (kcal/mol)	r_0 (Å)	ω_X (cm^{-1})	E_{act} (kcal/mol)	ΔE_{act}[a] (kcal/mol)	A_H/A_D	KIE (30 °C)
WT-SLO	6	19.5	0.57	–	2.1	1.0	16.1	84
$Leu^{546} \rightarrow Ala$	6	30	0.57	–	4.6	1.0	17.7	87
$Leu^{754} \rightarrow Ala$	6	36	0.57	–	6.0	0.9	18.2	88
$Ile^{553} \rightarrow Ala$	6	19.5	1.0	–	2.5	5.0	89	3.3×10^5
WT-SLO	6	19.5	0.6	400	2.8	1.2	12.4	93
$Leu^{546} \rightarrow Ala$	6	19.5	0.7	165	4.0	1.9	4.1	91
$Leu^{754} \rightarrow Ala$	6	19.5	0.7	165	4.0	1.9	4.1	91
$Ile^{553} \rightarrow Ala$	6	19.5	1.0[b]	89	8.1	3.0	0.57	85

[a] This is the isotope effect on E_{act}, $\Delta E_{act} = E_{act}D - E_{act}H$. [b] The effective Δr is 0.6 Å for H and 0.53 Å for D at 303 K.

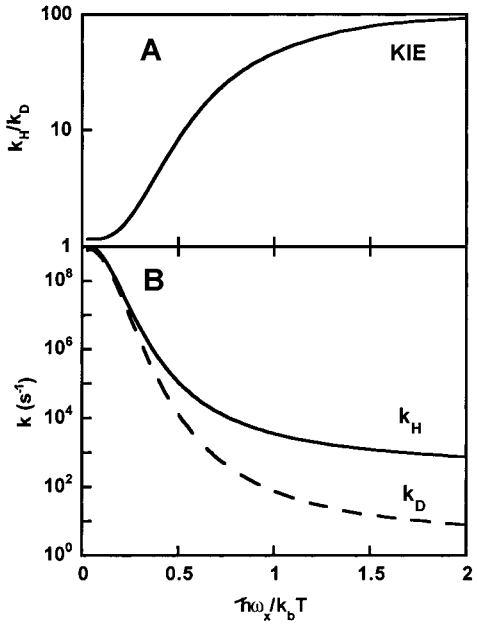

Figure 3. Calculated rates and KIEs for environmentally modulated H· and D· tunneling as a function of gating frequency at 303 K. See text for details.

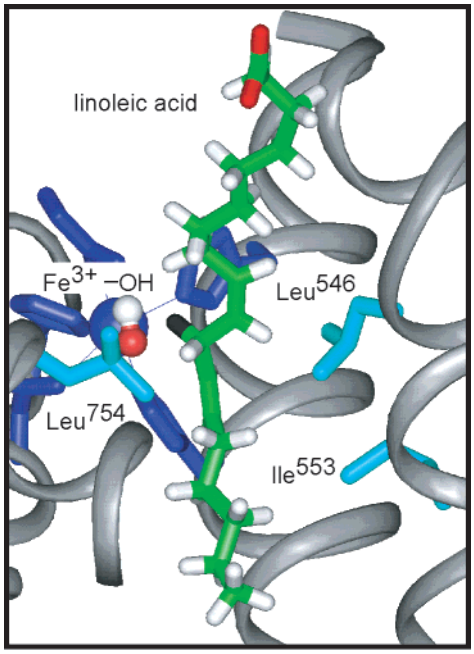

Figure 4. Model of linoleic acid in the crystal structure of SLO. Fe^{3+} and its protein-derived ligands (indigo); the hydroxo-ligand (red/white); LA (green/red/white), with the pro-S hydrogen (black) of C-11; and Leu^{546}, Leu^{754}, and Ile^{553} (cyan) are illustrated.

of gating on the temperature dependence of the isotope effect, isotope effects were simulated while varying the gating energy. The gating vibration was treated as a simple harmonic oscillator[13] of a mass that corresponds to an amino acid side chain (110 g/mol). A plot of the relationship between k_H or k_D (k_{cat} for the respective isotope) and the KIE, with the gating vibrational energy (normalized to thermal energy, k_bT), is shown in Figure 3. In this simulation, the reorganization energy was fixed at $\lambda = 18$ kcal/mol, $-\Delta G° = 6$ kcal/mol, $|V_{el}| = 0.14$ kcal/mol, and $r_0 = 1.0$ Å. The gating energy ($^1/_2\hbar\omega_x X^2$) was varied by changing the frequency of the gating vibration (ω_X) while holding the temperature fixed at 300 K. The size and the temperature dependence of the KIE are sensitive to the temperature-normalized frequency of the gating vibration. When the gating vibrational energy is much greater than thermal energy ($\hbar\omega_X/k_bT \gg 1$), the KIE is weakly temperature dependent; in the opposite limit ($\hbar\omega_X/k_bT \ll 1$), the KIE is markedly temperature dependent.

Hydrogen tunneling in which gating was ignored accounted for the data from WT-SLO very well and could also account for the data from the two distal mutants ($Leu^{546} \rightarrow$ Ala and $Leu^{754} \rightarrow$ Ala) reasonably well, by assuming an H· transfer distance of 0.567 Å. However, the $Ile^{553} \rightarrow$ Ala mutant exhibits a significantly temperature-dependent KIE, which could not be adequately modeled by this treatment. The gated model of hydrogen tunneling reproduced the trends in the data from WT-SLO and the mutants; the simulation parameters are listed in Table 2. The lack of agreement of E_{act} for $Ile^{553} \rightarrow$ Ala with experiment may reflect a lower λ for this mutant. Importantly, these simulations demonstrate how a reduced gating frequency leads to a more temperature-dependent KIE.

Discussion

Mutations Affect Hydrogen Transfer. Many bulky, aliphatic residues comprise the substrate-binding pocket of SLO.[36] The three residues which are the focus of this study, Leu^{546}, Leu^{754}, and Ile^{553}, are near the active site Fe (Figure 4). Modeling of LA into the binding pocket indicates that Leu^{546} and Leu^{754} lay within 6 Å of the Fe^{3+}-OH and are near the reactive C-11 of LA. Ile^{553} is more distant from the Fe^{3+}-OH, at 9 Å away, but still forms part of the substrate-binding cavity. Each of these residues provides a large surface to interact with bound substrate, particularly Leu^{546} and Leu^{754}.

Mutating a large Ile or Leu side chain to an Ala side chain opens up space within the binding pocket of SLO, leading to altered H· transfer kinetics. The $Leu^{546} \rightarrow$ Ala mutant decreases

(36) Minor, W.; Steczko, J.; Stec, B.; Otwinowski, Z.; Bolin, J. T.; Walter, R.; Axelrod, B. *Biochemistry* **1996**, *35*, 10687−10701.

k_{cat} by 60-fold from WT, while Leu^{754} → Ala decreases k_{cat} by 1000-fold, indicating that these hydrophobic residues contribute significantly to catalysis. The decreased rates for these mutants are attributed to altered heavy-atom motions (cf. Table 2 and Discussion below) that lead to increased energies of activation (Table 1). One can make arguments analogous to those used in discussing transition-state stabilization that relate changes in rate to changes in the free energy of activation. For k_{cat}/K_M, the change in free energy for converting free enzyme and substrate to the reactive configuration can be compared for WT-SLO and the three mutants of SLO (eq 3).[37]

$$\Delta\Delta G^{\ddagger} = -RT \ln \frac{(k_{cat}/K_M)_{mutant}}{(k_{cat}/K_M)_{WT}} \quad (3)$$

In this scenario, $\Delta\Delta G^{\ddagger}$ is the difference in the heavy-atom activation barrier for the reaction catalyzed by a given mutant relative to the reaction catalyzed by WT-SLO. The calculated free energy difference from k_{cat}/K_M values for the mutants, $\Delta\Delta G^{\ddagger}$, reflects the differential stabilization of the reactive configuration by mutant enzyme relative to WT and is very similar to the increase in E_{act} observed for these mutants from k_{cat} measurements (Table 1). This result argues against a change in substrate binding energy as the origin of the reduced rates observed in these mutants. A temperature-dependent conformational change in free enzyme can also be excluded as the origin of the reduced rates in these mutants, as this would affect k_{cat}/K_M while not affecting k_{cat}. It is possible that the observed increase in E_{act} reflects a temperature-dependent equilibrium between a dominant, inactive form of the enzyme−substrate complex and the active form; however, this can be viewed as an extreme case of an environmental reorganization that precedes the tunneling event.

Ile^{553} is roughly one helical turn distant from Leu^{546} in the LA binding pocket, and more remote from the Fe^{3+}-OH. The finding that k_{cat} and the corresponding E_{act} are unchanged from WT-SLO (Table 1) indicates that any alteration in the environmental coordinates due to the Ile^{553} → Ala mutation is not manifest on H· transfer. By contrast, D· transfer is significantly more temperature dependent than in WT-SLO (Figure 1), leading to a substantially more temperature-dependent KIE. Clearly, a comprehensive tunneling model that accounts for changing temperature-dependencies of KIEs is needed to explain the behavior of this mutant SLO in relation to WT-SLO and the other mutants (Table 1). Environmentally modulated hydrogen tunneling provides such a model.

Environmentally Modulated Hydrogen Tunneling. The Marcus electron-transfer (ET) model[30] considers the environmental coordinate, and the free energy of activation resulting from its driving force ($\Delta G°$) and its reorganization energy (λ), as dominant in determining the rate of ETs. In Marcus's model, the quantum particle (e^-) tunnels once environmental fluctuations allow the heavy nuclei to attain the reactive configuration. It is the probability of attaining this reactive configuration, not the rate of e^- tunneling, that dominates the rate of reaction, and the relevant potential energy surface for an electron-transfer reaction is the environmental surface.

Several workers have formulated hydrogen transfer reactions in a form resembling[10,25,32] the Marcus ET model, with the resultant rate expressions showing a dependence upon $\Delta G°$, λ, and the nuclear overlap along the hydrogen coordinate. Kuznetsov and Ulstrup[13] formulated hydrogen transfer reactions from an analytical approach similar to Jortner's treatment of nonadiabatic reactions.[38] This atom-transfer model has its origins in the earlier model[39] of Dogonadze, Kuznetsov, and Levich, which was summarized in a recent review.[40] This approach relies upon separating out the faster quantum coordinates (e- and H) from the slower environmental coordinate. Many well-characterized properties of hydrogen transfers, such as an inverted region in the free-energy dependence of the transfer rate, as well as a free-energy dependence to the KIE, follow from this Marcus-like model.[40] Absent gating, this model predicts similar E_{act} for both H· and D· transfer, such that the resultant KIE is only slightly temperature dependent, producing elevated Arrhenius prefactor ratios ($A_H/A_D \gg 1$).

A key rate determinant for hydrogen tunneling is the distance of hydrogen transfer, with the isotope effect reflecting the stronger distance dependence of deuterium tunneling than that of protium tunneling. In this context, hydrogen transfer rates are expected to be sensitive to any modulation of the transfer distance that creates a dynamic tunneling barrier. Thus, there are two types of environmental oscillations that modulate hydrogen transfer: fluctuations that lead to the reactive configuration along the environmental coordinate, and fluctuations that modulate the distance of H· transfer. Those fluctuations along the environmental coordinate are parametrized by λ and can be thought of as "passive dynamics" in the sense that they do not actively modulate the hydrogen tunneling probability; rather they control the probability of attaining a configuration from which tunneling is possible. Modulation of the transfer distance by gating has the effect of linking environmental dynamics to the hydrogen transfer and can be thought of as "active dynamics". The effect of these active dynamics on isotope effects was explored via simulations.

Simulations of rates and the KIEs, according to the gated hydrogen transfer model (eqs 1, 2b), are shown in Figure 3 to illustrate the global trends. When the experimentally accessible temperature range is small, the temperature dependence of the rates and KIEs appear linear, giving an Arrhenius-like rate (tangent to the calculated curves) in a semilog Arrhenius plot. The apparent temperature dependence of the rates and KIEs will reflect the rigidity of these active dynamics; for a large gating energy ($\hbar\omega_x > k_bT$), active dynamics are effectively frozen and modulate the H· or D· transfer very little. The rates of hydrogen transfer are then determined largely by the free energy barrier to reaction ($\Delta G°$ and λ). The KIEs are very large and weakly temperature dependent in this "stiff" regime.

This model predicts that the rate of reaction and the KIE will become more temperature dependent as the gating energy decreases ($\hbar\omega_X < k_bT$) and modulates the tunneling distance. In this regime, there is sufficient thermal energy to excite environmental modes that actively modulate the tunneling barrier. Other models predict similar trends in the rate of H· transfer;[10,25] however, no predictions were made of the KIEs.

(37) Fersht, A. *Enzyme Structure and Mechanism*, 2nd ed.; W. H. Freeman: New York, 1985.

(38) Jortner, J.; Ulstrup, J. *Chem. Phys. Lett.* **1979**, *63*, 236−239.
(39) Levich, V. G.; Dogonadze, R. R.; German, E. D.; Kuznetsov, A. M.; Kharkats, Y. I. *Electrochim. Acta* **1970**, *15*, 353−367.
(40) Krishtalik, L. I. *Biochim. Biophys. Acta* **2000**, *1458*, 6−27.

In this model, environmental dynamics modulate hydrogen tunneling because gating reduces the hydrogen potential well separation from an initial distance, r_0, to the final tunneling distance, $\Delta r = r_0 - r_X$. The increased tunneling probability at very short distance is offset by the decreased probability of attaining the short transfer distances. Reducing the transfer distance requires thermal energy in the gating coordinate, making the resultant tunneling distance, Δr, temperature dependent. This leads to a "compromise" transfer distance that will be different for H· and D·, leading to a temperature-dependent KIE and reduced A_H/A_D ratio; the smaller the gating frequency, the smaller this ratio becomes, until it ultimately becomes inverse ($A_H/A_D < 1$).

Simulations of the Data. The KIE parameters for WT-SLO can be accounted for by neglecting gating (Table 2). In this calculation, $r_0 = 0.567$ Å, the driving force is $\Delta G° = -6$ kcal/mol, $\lambda = 19.5$ kcal/mol, and gating is not operative. This predicts a weakly temperature-dependent KIE (84 at 303 K), with a low activation energy for both H· and D· transfer, and $\Delta E_{act} = 1.0$ kcal/mol; prior workers used similar parameters[13] to simulate the room-temperature KIE of WT-SLO. This simulation predicts a large Arrhenius prefactor ratio, $A_H/A_D = 16$. One difficulty with this treatment is that it requires that the substrate be bound at a close transfer distance, with the donor carbon atom and acceptor oxygen atom at a distance of 2.8 Å, ca. 0.6 Å less than van der Waals contact. It is possible that extensive binding energies within the [ES] complex permit such a close approach, and selected computational studies of reactive C−H−−O[41] and C−H−−C[42] interactions support such a possibility. However, we consider it more likely that this derived distance may be a consequence of the assignment of ω_H, to a harmonic stretching frequency, together with the treatment of this reaction as nonadiabatic, and that the actual distance of transfer is somewhat longer.

Equally good simulations of the data for WT-SLO were obtained with the active-dynamics model, in which $r_0 = 0.60$ Å, and $\Delta G°$ and λ are as above, by incorporating a stiff gating frequency, $\omega_X = 400$ cm^{-1}. Such high-energy gating modulates the hydrogen transfer distance to a very small extent. Within the context of Figure 3, this would correspond to $\hbar\omega_X/k_bT \approx 2$. Both of these simulations are within reasonable agreement of the experimentally measured KIE data for WT-SLO; consequently, we attribute the WT-SLO data to an active site that is highly preorganized, in which the passive dynamics[43] of environmental reorganization are important. This can be structurally rationalized as the binding site for LA is nonpolar, which should reduce λ, and very constricted, making active dynamics (gating) energetically costly. It appears that the reaction coordinate for WT-SLO is dominated by the environmental coordinate ($\Delta G°$ and λ) and that gating plays a minor role. The X → Ala mutants open up space within this binding pocket, changing this optimized condition.

Modeling of the data for Leu^{546} → Ala and Leu^{754} → Ala without gating utilized identical parameters as for WT-SLO, but with an increased reorganization energy ($\lambda = 30$, 36 kcal/mol, respectively). Increasing λ increases the calculated E_{act} for H· transfer, while retaining a nearly temperature-independent KIE as seen in WT-SLO. Simply increasing the transfer distance (r_0) resulted in an increased KIE, contrary to experimental observation. Using an increased λ is equivalent to the arguments above regarding decreased stabilization of the reactive configuration and reflects "passive dynamics", which are involved in attaining the reactive configuration along the environmental coordinate.

Both of these mutants are less optimized than WT-SLO, as shown by their reduced rates, which may be due to increased λ. However, simply increasing λ does not accommodate the reduced isotope effect on the Arrhenius prefactor ratio (A_H/A_D), which suggests that gating may be more relevant in these mutants than in WT-SLO. The properties of both of these mutants could, thus, be accounted for within the gated tunneling model by using a larger transfer distance ($r_0 = 0.70$ Å) and a softer gating vibration, $\omega_X = 165$ cm^{-1}, which corresponds to $\hbar\omega_X/k_bT \approx 0.8$ in Figure 3. This resulted in simulations that reproduced all of the experimental KIE data, including the Arrhenius prefactor isotope ratios. It appears that these mutations lead to a hydrogen transfer coordinate that is less preorganized than that in WT-SLO, leading to a larger gating contribution. This suggests that these mutations relax the active site, widening the hydrogen transfer distance to some extent, while also softening the gating vibration.

The isotope-effect pattern for the Ile^{553} → Ala mutant, a large ΔE_{act} and the inverse A_H/A_D ratio, cannot be accounted for without gating. A nongated tunneling model cannot simultaneously accommodate the observed KIE magnitude and temperature dependence (Table 2). The only way to obtain an inverse A_H/A_D ratio is to allow for a small gating energy, such that gating is thermally active. KIEs that are large, but with inverse A_H/A_D ratios, are calculated for a longer equilibrium H· separation distance, $r_0 = 1.0$ Å, and smaller gating frequency, $\omega_X = 89$ cm^{-1}, which corresponds to $\hbar\omega_X/k_bT \approx 0.4$ in Figure 3. These simulations result in a temperature-dependent KIE, characterized by $\Delta E_{act} = 3.0$ kcal/mol, and $A_H/A_D = 0.57$, values which approach those observed for Ile^{553} → Ala. The active gating coordinate results in calculated H· and D· transfer distances of 0.60 and 0.53 Å at 30 °C, respectively; these values are temperature dependent. That hydrogen tunneling is gated suggests that the active-site of the Ile^{553} → Ala mutant is much less rigid than that of WT-SLO, such that the barrier to tunneling is wider. The loss of rigidity allows for environmental gating to modulate this barrier; this is "active dynamics".

A structural rationalization for the onset of gating in the Ile^{553} → Ala mutant is possible if this mutation alters hydrophobic packing within the active site. X-ray crystallography could provide some insight into this, as would molecular dynamics studies. This mutation, which is more distant from the reactive C-11 of LA than the proximal Leu^{546} and Leu^{754} residues, may perturb packing in a critical region of the protein, leading to altered protein−substrate contacts. This may result in a reactive configuration along the environmental coordinate that has a longer hydrogen transfer distance than in WT-SLO (1.0 Å vs 0.6 Å), that is, an active site that has become less compressed.

(41) Himo, F.; Eriksson, L. A.; Maseras, F.; Siegbahn, P. E. M. *J. Am. Chem. Soc.* **2000**, *122*, 8031−8036.
(42) Camaioni, D. M.; Autrey, S. T.; Salinas, T. B.; Franz, J. A. *J. Am. Chem. Soc.* **1996**, *118*, 2013−2022.
(43) The active and passive dynamics mentioned here are similar to the symmetric and antisymmetric vibrations, respectively, discussed by Schwartz and co-workers. (a) Antoniou, D.; Schwartz, S. D. *J. Chem. Phys.* **1996**, *104*, 3526−3530. (b) Antoniou, D.; Schwartz, S. D. *Proc. Natl. Acad. Sci. U.S.A.* **1997**, *94*, 12360−12365. (c) Antoniou, D.; Schwartz, S. D. *J. Chem. Phys.* **1998**, *108*, 3620−3625. (d) Antoniou, D.; Schwartz, S. D. *J. Phys. Chem. B* **2001**, *105*, 5553−5558.

Table 3. KIE Patterns for Static and Environmentally Coupled Models of Hydrogen Tunneling

region	magnitude of A_H/A_D	description of tunneling	k_H/k_D	E_{act}	ΔE_{act} ($E_{act}D - E_{act}H$)
		static model, variable amount of tunneling			
IV	$\gg 1$	extensive	enormous	0	$E_{act}H = E_{act}D$
II	$\ll 1$	moderate	elevated	>0	$E_{act}H \ll E_{act}D$
I or III	≈ 1	classical behavior, or transition between extensive and moderate tunneling	variable	>0	$E_{act}H < E_{act}D$
		dynamic model, full tunneling			
IV	$\gg 1$	passive dynamics dominant	very large to moderate	>0	$E_{act}H \approx E_{act}D$
II	$\ll 1$	active dynamics dominant	wide range possible	$\gg 0$	$E_{act}H \ll E_{act}D$
I or III	≈ 1	transfer over the barrier, or a transition between the above two regions	variable	$\gg 0$	$E_{act}H < E_{act}D$

At this less optimized reactive configuration, modulation of the tunneling distance by environmental dynamics becomes a requirement.

This gating model can fully account for the isotope effect pattern observed in WT-SLO and all three mutants; however, it fails to reproduce the E_{act} observed in the Ile^{553} → Ala mutant (Tables 1 and 2). In other words, the dynamic model predicts the differences between H· and D· transfer rates very well, but it fails to reproduce the absolute temperature dependence of the individual rates for this one mutant. As noted earlier, this discrepancy could be resolved if λ for Ile^{553} → Ala were reduced relative to WT-SLO. Alternatively, this may reflect both the complexity of tunneling barriers and the simplicity of the gating model. In this model, we have assumed that the hydrogen tunnels between diabatic (unmixed) harmonic oscillators of equivalent frequency. Although more complex barrier shapes were not accounted for, it is unlikely that these alone could account for the observed temperature dependence of the KIE, particularly the inverse A_H/A_D ratio. However, the very simple gating model neglects changes in the shape of the tunneling barrier due to gating. Changing the barrier shape would alter the tunneling probability of H· and D· to different extents and would require an explicit coupling between the gating dynamics and the hydrogen wave function. While several theoretical groups are working on this problem,[20,44] it is beyond the scope of the current analysis.

Relation to Other Tunneling Proposals. Several groups have proposed hydrogen transfer models that require environmental oscillations to modulate the tunneling barrier. The model used here is very similar to that presented by Borgis and Hynes,[10,25,32,45] in that environmental fluctuations modulate the hydrogen tunneling overlap. Schwartz's approach builds on the Borgis and Hynes model to allow tunneling from excited states,[46] as well as to incorporate molecular dynamics simulations to look for rate-promoting vibrations.[47] That approach has the advantage of treating environmental motions that are highly quantized and, thus, accounts for the amplitude of zero-point oscillations that can lead to significant effects. For example, a quantum-mechanical treatment of the gating vibration in WT-SLO would incorporate the zero-point vibration, leading to a finite oscillation amplitude even at low temperature. This same gating vibration, when treated classically (as in this work), requires thermal activation to attain any oscillation amplitude. Thus, our classical treatment essentially turns off the gating oscillation by increasing its frequency (equivalent to an increased force constant), whereas a quantized treatment of gating would retain a minimal zero-point amplitude.

Bruno and Bialek[11] proposed an early treatment of hydrogen transfer promoted by environmental vibrations − vibrationally enhanced ground-state tunneling (VEGST). This model was developed to account for nonclassical KIEs observed in the copper amine oxidase,[48] specifically, a very temperature-dependent KIE in a tunneling reaction. By coupling environmental motion to hydrogen tunneling, they were able to account for a fully quantum-mechanical hydrogen transfer that had appreciable temperature dependence. Thus, the hallmarks of VEGST are temperature-dependent KIEs in a hydrogen tunneling reaction; in other words, $A_H/A_D \leq 1$. In this regard, VEGST and gated hydrogen tunneling are the same model, despite the fact that several of the parameters are defined differently.

Several recent reports of temperature-independent KIEs and $A_H/A_D > 1$, as observed in WT-SLO, have been suggested as evidence for VEGST.[22,23] While such a KIE pattern can be accommodated by the VEGST model, this requires that the "vibrational enhancement" (or gating) is a minor part of the reaction. It seems inappropriate to use such instances as evidence for a role of rate-promoting vibrations in catalysis. As discussed for WT-SLO within the context of the gated tunneling model, such a KIE pattern is consistent with environmental reorganization dominating the reaction coordinate, but little or no gating. Thus, the dominant environmental contribution in WT-SLO is the environmental reorganization (passive dynamics), which is different from a vibrationally enhanced modulation of the tunneling probability (active dynamics). Modulation of tunneling via active dynamics requires that an environmental vibration has sufficient amplitude to alter the H-transfer coordinate; within the gating model, the gating mode must be thermally active ($\hbar\omega_x \leq k_bT$). This would lead to temperature-dependent KIEs and produce an inverse Arrhenius prefactor isotope effect ($A_H/A_D \ll 1$).

Temperature-Dependent KIEs in the Context of Gated Hydrogen Tunneling. We propose a new interpretation of hydrogen tunneling behavior on the basis of the environmentally modulated tunneling model discussed here. This behavior is

(44) Hammes-Schiffer, S. *Acc. Chem. Res.* **2001**, *34*, 273−281.
(45) Borgis, D.; Hynes, T. *J. Chim. Phys. Phys.-Chim. Biol.* **1990**, *87*, 819−829.
(46) Antoniou, D.; Schwartz, S. D. *J. Chem. Phys.* **1998**, *108*, 3620−3625.
(47) Antoniou, D.; Schwartz, S. D. *J. Phys. Chem. B* **2001**, *105*, 5553−5558.
(48) Grant, K. L.; Klinman, J. P. *Biochemistry* **1989**, *28*, 6597−6605.

contrasted to an earlier proposal (Table 3) that focused on the extent of tunneling versus classical reaction within a static model.[17] In this previous formalism, the reaction coordinate varied from purely classical (region I) to purely tunneling (region IV) with the attendant changes in the temperature dependence of the KIE. As discussed earlier, the behavior of WT-SLO is sufficiently extreme to require a full quantum-mechanical model. This full-tunneling model leads to a range of temperature dependencies for the KIEs, but reflects the extent to which gating modulates H· transfer in a full-tunneling model, rather than the extent of classical reaction.

In rigid environments ($\hbar\omega_x/k_bT \geq 1.4$), the gating vibration does not modulate the tunneling distance appreciably, leading to a nearly temperature-independent tunneling distance. This region IV behavior approaches static hydrogen tunneling, which has large KIEs that are temperature independent ($A_H/A_D > 1$), but differs from region IV in the earlier formalism since E_{act} can be appreciable due to the environmental reorganization energy. As the gating energy decreases, gating becomes more effective at modulating the tunneling probability. Region III ($1 \leq \hbar\omega_x/k_bT \leq 1.4$) is characterized by more temperature-dependent KIEs and by values for A_H/A_D that pass through unity. Significant gating is evident in region II ($0.4 \leq \hbar\omega_x/k_bT \leq 1$), where the gating frequency is reduced sufficiently to allow a more temperature-dependent tunneling distance, resulting in KIEs that are so temperature dependent that $A_H/A_D < 1$ is predicted. Finally, in region I ($\hbar\omega_x/k_bT \leq 0.4$), extensive environmental dynamics lead to smaller KIEs that follow the classical prediction, with $A_H/A_D = 1$.

The observed isotope effect pattern in any given reaction proceeding by tunneling depends on the amount of thermal energy available for gating; if sufficient thermal energy is available, then tunneling is environmentally enhanced to a large degree (regions II and III). This model proposes that the hallmark of either VEGST or gated tunneling is a temperature-dependent KIE, with $A_H/A_D \leq 1$. The temperature-independent KIEs and $A_H/A_D \gg 1$ observed for WT-SLO are consistent with a highly organized and stiff active site, leading to a reaction that proceeds fully by hydrogen tunneling with little modulation by gating. The more temperature-dependent KIEs of the Leu^{754} → Ala and Leu^{546} → Ala mutants are consistent with a softer active site and, consequently, a hydrogen transfer that proceeds with a modest degree of environmental gating. The curious observation of highly temperature-dependent KIEs and $A_H/A_D \ll 1$ in the Ile^{553} → Ala mutant is indicative of extensive gating that modulates the hydrogen tunneling reaction. These results indicate that modest changes in protein structure can introduce the need for active dynamics to generate a suitable barrier for tunneling in soybean lipoxygenase-1.

Concluding Comments

Through a combination of temperature-dependent isotope effects and mutagenesis, we have probed the link between enzyme catalysis and dynamics in SLO. This study presents data that are inconsistent with simple classical models of catalysis, requiring catalytic models that invoke environmentally modulated hydrogen tunneling under ambient conditions. KIEs provide a powerful probe for detection of environmentally promoted tunneling, and their use is altering our understanding of enzyme catalysis. A new interpretation of the previously[17] proposed "tunneling-regions diagram" is that the temperature dependence of KIEs reflects the degree to which active environmental dynamics (gating) promote catalysis. WT-SLO exhibits parameters consistent with "region IV" behavior: nearly temperature-independent KIEs, with $A_H/A_D \gg 1$, reflecting little involvement of active dynamics to promote catalysis. The Leu^{754} → Ala and Leu^{546} → Ala mutants exhibit KIEs that approach "region III" behavior: temperature-dependent KIEs, with an A_H/A_D ratio that approaches unity, indicating a modest role of active dynamics to modulate hydrogen transfer. The Ile^{553} → Ala mutant, on the other hand, exhibits "region II" behavior: markedly temperature-dependent KIEs, with $A_H/A_D < 1$, reflecting a significant role for active dynamics to modulate the tunneling barrier in this mutant, that is, gating.

We expect our full tunneling analysis of SLO to be especially relevant for other enzymes that catalyze hydrogen-atom (H·) transfer, since these enzymes have fewer means to stabilize a classical transition state than do proton (H^+) or hydride (H^-) transfer enzymes. In such H· transfer reactions, modulation of reaction barrier shape and dynamics to enhance tunneling may dominate the catalytic process. Evaluating the importance of dynamic modulations of the reaction coordinate becomes possible through study of the temperature dependence of KIEs in these systems.

Acknowledgment. This research was supported by grants to J.P.K. from the NSF (MCB9816791) and the NIH (GM25765), and by NIH postdoctoral fellowships to M.J.K. (GM19843) and K.R. (GM17811). We thank Drs. S. Seymour, M. Meyer, and J. Roth (UCB) for stimulating discussions.

Appendix

Origin of the Analytical Rate Expressions. Our eq A1 (eq 1 in the main text) is a combination of eqs 12−16 from Kuznetsov and Ulstrup (Kuznetsov, A. M.; Ulstrup, J. *Can. J. Chem.* **1999**, *77*, 1085−1096). We used more conventional chemical nomenclature in our expression; therefore, the derivation of eq A1 is summarized below to facilitate comparison with the original derivation. Equation A1 describes the rate of hydrogen transfer in the presence of a classical environment as the sum of state-specific rates:

$$k_{tun} = \sum_v P_v \sum_w \frac{1}{2\pi} |V_{el}|^2 \sqrt{4\pi^3/\lambda RT\hbar^2}\, \exp^{-(\Delta G^\circ + E_{vib} + \lambda)^2/(4\lambda RT)} \times (\text{F.C. term})_{v,w} \quad \text{(A1)}$$

The rate is a sum over all level-specific rates, in which v is the vibrational quantum number for reactant, and w is the vibrational quantum number for product, that have been normalized for the thermal populations. The rate is determined by $|V_{el}|^2$, the electronic overlap of reactant and product squared, and an environmental energy term relating λ, the reorganization energy of classical modes, to ΔG°, the driving force for the reaction; E_{vib} is the difference in vibrational energy between the reactants and products. The hydrogen stretch is treated quantum mechanically, and its contribution to the rate is due to a vibration-level specific Franck−Condon overlap (F.C. term). Other symbols have their usual meaning: $\hbar$ is Planck's constant divided by 2π, and R and T are the gas constant and absolute temperature, respectively.

To arrive at A1, we begin with the total rate of reaction, k_{tun}, as a sum of each level-specific rate, $k_{\upsilon w}$ (eq A2), where P_υ is the boltzmann population of level υ. The thermal population of each initial state is determined by use of the vibrational partition function, in which $E_\upsilon = h\nu(\upsilon)$, as all energies are expressed relative to the $\upsilon = 0$ level:

$$k_{tun} = \sum_{\upsilon} \frac{\exp^{(-E_\upsilon/k_B T)} \sum_{w} k_{\upsilon w}}{\sum_{\upsilon} \exp^{(-E_\upsilon/k_B T)}} = \sum_{\upsilon} P_\upsilon \sum_{w} k_{\upsilon w} \qquad \text{(A2)}$$

where k_B is Boltzmann's constant, and $k_{\upsilon w}$ is the state-specific rate of reaction from initial state υ (reactant vibrational level) to final state w (product vibrational level) (eq A3).

$$k_{\upsilon w} = \kappa_{\upsilon w} \frac{\omega_{\text{eff}}}{2\pi} \exp^{-\Delta G_{\upsilon w}^{\ddagger}/RT} \qquad \text{(A3)}$$

The level-specific rate expression contains $\kappa_{\upsilon w}$, the transmission coefficient (defined below); ω_{eff}, a characteristic average frequency of the environmental modes that are treated classically; and $\Delta G^{\ddagger}$, the free energy barrier:

$$\Delta G_{\upsilon w}^{\ddagger} = (\lambda + \Delta G^{\circ} + E_{\text{vib}})^2/4\lambda \qquad \text{(A4)}$$

As defined above, λ is the reorganization energy of the classical modes, ΔG° is the free energy of reaction, and E_{vib} is the vibrational energy difference between the reactant level (υ) and product level (w). The latter term varies slightly for each transition (cf. Table S1).

The transmission coefficient ($\kappa_{\upsilon w}$) contains the electronic overlap term (V_{el}^2), the Franck−Condon term for overlap along the proton coordinate (F.C. term), as well as the familiar prefactor due to the classical environment.

$$\kappa_{\upsilon w} = \sqrt{4\pi^3/\lambda RT\hbar^2\omega_{\text{eff}}^2}(V_{\text{el}})^2(\text{F.C. term})_{\upsilon w} \qquad \text{(A5)}$$

Combining eqs A2−A5 results in eq A1.

Expressions for the Franck−Condon overlaps (F.C. term$_{\upsilon w}$) are readily available (cf. Ulstrup, J.; Jortner, J. *J. Chem. Phys.* **1975**, *63*, 4358−4368). We assumed that each transition occurs between harmonic oscillators of equal frequencies. All F.C. terms used in our calculations are shown below, for transitions from the $\upsilon = 0$ or 1 level of reactant to the $w = 0$, 1, 2, or 3 level of product. The nuclear overlap depends on the frequency (ω) and mass (m) of the oscillator, as well as on Δr, the separation between the minima of the initial and final wells.

$$\text{F.C. term}_{0,0} = \exp^{-m\omega\Delta r^2/2\hbar} \qquad \text{(A6)}$$

$$\text{F.C. term}_{0,1} = \exp^{-m\omega\Delta r^2/2\hbar}(m\omega\Delta r^2/2\hbar) \qquad \text{(A6)}$$

$$\text{F.C. term}_{0,2} = {}^1/_2 \exp^{-m\omega\Delta r^2/2\hbar}(m\omega\Delta r^2/2\hbar)^2 \qquad \text{(A6)}$$

$$\text{F.C. term}_{0,3} = {}^1/_6 \exp^{-m\omega\Delta r^2/2\hbar}(m\omega\Delta r^2/2\hbar)^3 \qquad \text{(A6)}$$

$$\text{F.C. term}_{1,0} = \exp^{-m\omega\Delta r^2/2\hbar}(m\omega\Delta r^2/2\hbar) \qquad \text{(A7)}$$

$$\text{F.C. term}_{1,1} = \exp^{-m\omega\Delta r^2/2\hbar}(1 - m\omega\Delta r^2/2\hbar)^2 \qquad \text{(A7)}$$

$$\text{F.C. term}_{1,2} = {}^1/_2 \exp^{-m\omega\Delta r^2/2\hbar}(m\omega\Delta r^2/2\hbar)(2 - m\omega\Delta r^2/2\hbar)^2 \qquad \text{(A7)}$$

$$\text{F.C. term}_{1,3} = {}^1/_6 \exp^{-m\omega\Delta r^2/2\hbar}(m\omega\Delta r^2/2\hbar)^2(3 - m\omega\Delta r^2/2\hbar)^2 \qquad \text{(A7)}$$

Supporting Information Available: Two figures showing the correction for subsaturating [O_2] on k_{cat} for WT-SLO and Ile$^{553}\rightarrow$Ala. One table showing the breakdown of H· and D· tunneling by vibrational levels. Tabulated values of k_{cat} (H· and D· transfer rates) versus T for WT-SLO and each mutant (PDF). This material is available free of charge via the Internet at http://pubs.acs.org.

JA012205T